Document downloaded from:

http://hdl.handle.net/10251/101708

This paper must be cited as:

Cortes-Lopez, V.; Blanes Campos, C.; Blasco Ivars, J.; Ortiz Sánchez, MC.; Aleixos Borrás, MN.; Mellado Arteche, M.; Cubero García, S.... (2017). Integration of simultaneous tactile sensing and visible and near-infrared reflectance spectroscopy in a robot gripper for mango quality assessment. Biosystems Engineering. 162:112-123. doi:10.1016/j.biosystemseng.2017.08.005

The final publication is available at

http://doi.org/10.1016/j.biosystemseng.2017.08.005

Copyright Elsevier

Additional Information

Integration of simultaneous tactile sensing and reflectance visible and near-infrared spectroscopy in a robot gripper for mango quality assessment

V. Cortés[1], C. Blanes[2], J. Blasco[3], C. Ortiz[4], N. Aleixos[5], M. Mellado[2], S. Cubero[3], P. Talens[1(*)]

1) Departamento de Tecnología de Alimentos. Universitat Politècnica de València. Camino de Vera, s/n, 46022 Valencia, Spain

2) Instituto de Automática e Informática Industrial, Universitat Politècnica de València, Camino de Vera s/n, 46022 Valencia, Spain

3) Centro de Agroingeniería. Instituto Valenciano de Investigaciones Agrarias (IVIA). Ctra. Moncada-Náquera Km 4.5, 46113, Moncada, Valencia (Spain)

4) Departamento de Ingeniería Rural y Agroalimentaria, Universitat Politècnica de València, Camino de Vera s/n, 46022 Valencia, Spain

5) Departamento de Ingeniería Gráfica. Universitat Politècnica de València. Camino de Vera, s/n, 46022 Valencia, Spain

*E-mail of the corresponding author: pautalens@tal.upv.es

ABSTRACT

Development of non-destructive tools for determining mango ripeness would improve the quality of industrial production of the postharvest processes. This study addresses the creation of a new sensor that combines the capability of obtaining simultaneously both mechanical and optical properties of the fruit. It has been integrated in a robot gripper that can handle the fruit obtaining non-destructive measurements of firmness, incorporating two spectrometer probes to simultaneously obtain reflectance properties of the visible and near-infrared, and two accelerometers attached to the rear side of two fingers. Partial least square regression was applied to different combinations of the spectra data obtained from

the different sensors to determine the combination that provides the best results. Best prediction of ripening index was achieved using both spectral measurements and two finger accelerometers signals, with R^2_p = 0.832 and RMSEP of 0.520. These results demonstrate that simultaneous measurement and analysis of the data fusion set improve the robot gripper features, allowing to assess the quality of the mangoes during pick and place processes.

Keywords: spectrometry; chemometrics; non-destructive sensor; tactile sensor; accelerometer

1. INTRODUCTION

Mango (*Mangifera indica L.*) is a tropical fruit marketed throughout the world with a very high economic importance (Luke, 2013; Calatrava, 2014) that is generally harvested a little earlier than the fully mature stage to avoid the onset of climacteric respiration during transportation to distant markets (Jha *et al.*, 2007). Therefore, mango requires a ripening period before it achieves the taste and texture desired at the time of consumption (Cortés *et al.*, 2016). The ripening process, and hence the organoleptic quality, is regulated by genetic and biochemical events that result in biochemical changes such as the biosynthesis of carotenoids (Mercadante & Rodriguez-Amaya, 1998), loss of ascorbic acid (Hernández *et al.*, 2006), increase in total soluble solids (Padda *et al.*, 2011); physical changes such as weight, size, shape, firmness and colour (Ornelas-Paz *et al.*, 2008; Kienzle *et al.*, 2011); and changes in aroma, nutritional content and flavour of the fruit (Giovannoni, 2004). The evaluation of these changes plays an important role for determining the ripening level of harvesting, which will decide the market (i.e. domestic, exportation) and/or price of the product. Traditional determination of these changes has required a destructive methodology using specialised equipment, procedures and trained personnel, which results in high analysis costs (Torres *et al.*, 2013). In addition, destructive methods allow to analyse only a few set of samples trying to represent the variability of the whole production, but this desirable situation can be only achieved if all fruits are inspected in automated lines (Kondo, 2010). Traditionally, electronic sorters based on computer vision, used in postharvest to inspect the quality of the fruit, work at a very high speed, analysing the surface of the fruits not being possible any internal inspection. The most advanced and innovative sorters can incorporate NIR technology for testing the internal properties of the produces but light is projected to the fruit at a fixed distance and later, the reflected or transmitted light, is also measured at a certain fixed distance. However, as the fruits have different sizes and shapes, the measurements can be strongly influenced by these features. For instance Velez-Rivera *et al.* (2014a) and (2014b) developed computer vision techniques to determine damages and ripeness of mango 'Manila' trough colour measurements.

Robots have enormous potential to automate production in the food sector (Blasco *et al.*, 2003; Wilson, 2010). Their main current function is to transport and manipulate objects but they have clear difficulties for handling soft and variable products (Bogue, 2009). Advances in new robot grippers are allowing their introduction in industrial and manufacturing systems for monitoring and controlling production (Tai *et al.*, 2016). Automation with robots, in primary packaging operations, makes possible to incorporate different sensors that can be used to assess fruits quality. Tactile sensors added to gripper fingers provide the capability to evaluate a product through physical contact (Lee, 1999) and have been used for classifying eggplants (Blanes *et al.*, 2015a) and to assess cv. 'Osteen' mangoes firmness (Blanes *et al.*, 2015b) with a good prediction performance of the PLS model (R^2_P = 0.760 and RMSEP = 17.989).

Visible and near-infrared spectroscopy combined with multivariate analysis has been widely used for quantitative determination of several internal properties or compounds, to determine ripeness, and to measure quality indices in fruits in general and in mango in particular (Schmilovitch *et al.*, 2000; Theanjumpol *et al.*, 2013; Jha *et al.*, 2013; Cortés *et al.*, 2016). Cortés *et al.* (2016) predicted, in a laboratory, the internal quality index for cv. 'Osteen' mangoes using visible and near-infrared spectrometry (VIS-NIR) obtaining good results with the full spectral range and some selected wavelengths (R^2_p = 0.833 and R^2_p = 0.815, respectively). Thus, incorporating the capability of performing spectral measurements to gripper fingers in combination with other sensors would multiply the possibilities of measuring internal fruit quality when the fruit is handled. However, this would require to develop sensor fusion techniques to obtain the maximum of the combined information of all the sensors avoiding redundancy (Cimander *et al.*, 2002).
Furthermore, sensor fusion enables rapid and economical in-line implementation for fruit quality assessment (Ignat *et al*., 2015). Multiple sensors have been widely used in a variety of fields. Steintmetz *et al*., (1999) developed a robotic quality inspection system for apples that included a colour camera and NIR spectroscopy to predict sugar content using sensor fusion techniques. Since then, significant food advances in the field of sensor fusion have been developed among computer vision and near-infrared spectroscopy to assess fish freshness (Huang *et al.*, 2016), fusion of impedance e-tongue and optical spectroscopy to determine the botanical origin of honey (Ulloa *et al.*, 2013), sensor fusion of electronic nose and acoustic sensor to improve the mango ripeness classification (Zakaria *et al.*, 2012) or fusion of electronic nose, near-infrared spectrometer and standard bioreactor probes to monitor yoghurt fermentation (Cimander *et al.*, 2002). Hitherto, examples of combination of signals from visible and near-infrared spectroscopy spectral data and tactile sensors in a robot gripper are inexistent. Therefore, getting a sensor fusion

system integrating tactile and spectral properties of the fruit would be a key advance for the post-harvest industry.

Thus, the aim of this study is to develop a novel robotic gripper that incorporates accelerometers and fibre-optic probes coupled to a spectrometer to analyse the mango ripening state by simultaneously measuring firmness and visible and near-infrared reflectance when the fruit is handled in the packing house during postharvest operations.

2. MATERIALS AND METHODS

2.1. Experimental procedure

A batch of 275 unripe mangoes (*Mangifera indica* L., cv 'Tommy Atkins') were selected with similar size and colour and free of external damage. During the experiments, fruits were ripened in a storage chamber at 20.0 ± 2.1 ºC and 67.6 ± 3.3 % RH and fruits were divided in sets of 45 fruits each (sets marked as M1, M2, M3, M4, M5 and M6). Every 2-3 days one set was analysed starting with set M1 until the last set M6 reached senescence (18 days). All the mangoes in each set were handled by the robotic gripper to obtain non-destructive measurements and later their physicochemical properties (total soluble solids, titratable acidity and destructive firmness) were evaluated. Prior the measurements, the temperature of the mangoes was stabilised at 24 ± 1 ºC.

2.2. Reference analysis

Routine methods were used to determine the quality attributes of the mangoes. Mango firmness was measured using a Universal Testing Machine (TextureAnalyser-XT2, Stable MicroSystems (SMS) Haslemere, England) through a puncture tests using a 6 mm diameter cylindrical probe (P/15ANAMEsignature) until a relative deformation of 30 %, at a speed of 1 mm s^{-1}. Two measurements were performed per fruit, on opposite sides along the equator. The fracture strength (F_{max}) expressed in Newtons was also obtained for all samples.

The total soluble solids (*TSS*) content was determined by refractometry (%) with a digital refractometer (set RFM330+, VWR International Eurolab S.L Barcelona, Spain) at 20 ºC with a sensitivity of ± 0.1 ºBrix. Samples were analysed by triplicate.

The analysis of the titratable acidity (*TA*) was performed with an automatic titrator (CRISON, pH-burette 24, Barcelona, Spain) with 0.5 N NaOH until a pH of 8.1 (UNE34211:1981), using 15 g of crushed mango which was diluted in 60 mL of distilled water. The *TA* was determined based on the percentage of citric acid that was calculated using Eq. (1).

$$TA\ [g\ citric\ acid/100\ g\ of sample] = \left(\left((A \times B \times C) \cdot D^{-1}\right) \times 100\right) \cdot E^{-1} \qquad (1)$$

where *A* is the volume of NaOH consumed in the titration (in L), *B* is the normality of NaOH (0.5 N), *C* is the molecular weight of citric acid (192.1 g·mol^{-1}), *D* is the weight of the sample (15 g) and *E* is the valence of citric acid (*E* = 3).

A multi-parameter ripening index (*RPI*) was calculated by Eq. (2) which was described previously by Vásquez-Caicedo *et al.* (2005) and Vélez-Rivera *et al.* (2014b). This index was then used as reference to test the measurements obtained by the robot gripper:

$$RPI = ln(100 \cdot F_{max} \cdot TA \cdot TSS^{-1}) \qquad (2)$$

where F_{max} is the fracture strength (Newton), *TSS* is the total soluble solids (g soluble solids per 100 g of sample) and *TA* is the titratable acidity (g citric acid equivalent per 100 g of sample).

2.3. Robot gripper

A robot gripper has been specifically developed to handle quasi spherical fruit and programmed in these experiments to work with mango fruits. The gripper has four fingers: *FA1*, *FA2*, *FB1* and *FB2* (Fig. 1). The design of the gripper fingers and its mechanical configuration adapt to a wide range of varied shapes while are handled, and provide a good performance of the accelerometers as intrinsic tactile sensors (Blanes *et al.*, 2016). The *FA2* has hemispherical concave shape, is attached to the chassis of the gripper and is linked by a ball joint. The *FA1* is linked to a pneumatic cylinder (DSN 10-80P, Festo, Germany) with a float joint and has straight motion that is aligned with the *FA2*. The *FB1* and *FB2* are linked to their respective pneumatic cylinders (CD85N10-50B, SMC, Japan) with two float joints and move following parallel paths. *FA1*, *FB1* and *FB2* have pads of a latex membrane filled with sesame seeds. Each pad is soft when its internal pressure is atmospheric or slightly higher and tough when its internal pressure is lower than atmospheric. The design of these fingers allows the gripper adapting to every mango shape while it is grasped. The gripper was attached to a delta robot (IRB 340, Flexpicker, ABB, Switzerland).

In addition, the gripper was equipped with two types of sensors, two accelerometers (*ACC1* and *ACC2*) and two reflectance probes (*P1* and *P2*). The signals captured by the sensors were recorded in a laptop by means of a data acquisition module (USB 6210, National Instruments, USA) in the case of accelerometers, and a multichannel VIS-NIR spectrometer platform (AVS-DESKTOP-USB2, Avantes BV, The Netherlands) for the reflectance probes (Fig. 2)..

Accelerometers *ACC1* and *ACC2* were joined to the rear side of the *FA1* and *FA2* respectively. They are intrinsic tactile sensors because they are not in direct contact to every manipulated mango. *P2* was attached to the *FA2* through a hole performed in this finger. It was able to collect data as soon as both *FA1* and *FA2* were closed. Once *FA1* and *FA2* grasp a mango, *P1* approximates by means of the pneumatic cylinder action (C85E10-40, SMC, Japan). This probe was linked to the pneumatic cylinder rod by means of a ball joint. Ball joints allowed the probes adapting to the shape of every different mango since they can rotate freely around three rotation axes.

Due to the mechanical configuration of the gripper, the sensors took measurements at different points over the surface of every mango (Fig. 3).

2.3.1. VIS-NIR reflectance signals

Each reflectance probe consisting of seven fibres with a diameter of 200 µm, delivered the light to the sample through a bundle of six fibres, collecting the reflected light trough the seventh one. The probe tip was designed to provide reflectance measurements at an angle of 45° so as to avoid specular reflectance from the surface of the fruit.

The spectra of mango samples were collected in reflectance mode using the multichannel spectrometer platform equipped with two detectors and a quartz beam splitter (BSC-DA, Avantes BV, The Netherlands). The first detector (AvaSpec-ULS2048 StarLine, Avantes BV, The Netherlands) included a 2048-pixel charge-coupled device (CCD) sensor (SONY ILX554, SONY Corp., Japan), 50 µm entrance slit and a 600 lines mm^{-1} diffraction grating covering the working visible and near-infrared (VNIR) range from 600 nm to 1100 nm with a spectral FWHM (full width at half maximum) resolution of 1.15 nm. The spectral sampling interval was 0.255 nm. The second detector (AvaSpec-NIR256-1.7 NIRLine, Avantes BV, The Netherlands) was equipped with a 256 pixel non-cooled InGaAs (Indium Gallium Arsenide) sensor (Hamamatsu 92xx, Hamamatsu Photonics K.K., Japan), a 100 µm entrance slit and a 200 lines mm^{-1} diffraction grating covering the working NIR range from 900 nm to 1750 nm and a spectral FWHM resolution of 12 nm. The spectral sampling interval was 3.535 nm. Two Y-shaped fibre-optic reflectance probes (*P1* and *P2*) (FCR-7IR200-2-45-ME, Avantes BV, The Netherlands) were configured each with an illumination leg which connects the fibre-optic probe coupled to stabilised 10 W tungsten halogen light sources (AvaLight-HAL-S, Avantes BV, The Netherlands). The light sources ensure a permanent light intensity over the whole measurement range. The other leg of the Y-fibre-optic probe was connected to a beam combiner (BSC-DA, Avantes BV, The Netherlands) which converted the two light beams into one light beam. This only light beam was transmitted through another Y-shaped fibre-optic probe to both detectors for simultaneous measurement.

The calibration was performed using a 99 % reflective white reference tile (WS-2, Avantes BV, The Netherlands) so that the maximum reflectance value over the range of wavelengths was around 90 % of saturation. The integration time was set to 240 ms for the VNIR detector and to 4200 ms for the NIR detector due the different features of both detectors. For both detectors, each spectrum was obtained as the average of five scans to reduce the thermal noise of the detector (Nicolaï *et al.*, 2007). The average reflectance measurements of each sample (S) were then converted into relative reflectance values (R) with respect to the white reference using dark reflectance values (D) and the reflectance values of the white reference (W), as shown in Eq. (3):

$$R = \frac{S-D}{W-D} \qquad (3)$$

The dark spectrum was obtained by turning off the light source and completely covering the tip of the reflectance probe.

2.3.2. Accelerometers signals

The accelerometers used (ADXL278, Analog Devices, USA) have a measurement range of +/- 50 g. They are capable of sensing collisions and, motoring and control vibration.

Only the deceleration signals of the normal axes to the fingers were collected. They were sampled during approximately 0.27 s at 30 kHz and low-pass filtered (Fig. 4a), but only less than 0.1 s were used for analysing the tactile sensor responses. These signals were only processed between t_0 (0.0366 s) and t_1 (0.08 s) (Fig. 4b) to capture the first contacts of the gripper fingers with every mango. Signals were rearranged using the maximum values as reference, for hence always maximum values will be at 0.0125 s. Signals also were cut to collect 0.0315 s (Fig. 4c) and were transformed by Fast Fourier Transform using LabVIEW 11.0 (National Instruments, USA), with the option measurement magnitude root main square with Hanning window, in order to get energy spreading into frequencies (Fig. 4d).

2.4. Robot gripper process and signals acquisition

A robot program controls every grasping and sensing operation of the gripper. Three electrovalves (SY3120, SMC, Japan) were used, one for the motion of *FA1*, one the motion of *FB1* and *FB2* and other for moving the *P2*. Two adjustable flowmeter control valves (AS2201F-01-04S, SMC, Japan) were used to adjust the speed of *FA1* and *P2*. A vacuum generator with blow function (VN-07-H-T3-PQ2-VQ2-RO1-B, Festo, Germany) provides the possibility of controlling the hardness of *FA1* by means of its internal valves 2 and 4. The data acquisition device used to collect the accelerometer signals starts to collect data when the robot sends the signal to close *FA1*.

When the gripper is at the approach position to grasp a mango, valve 1 is activated for closing *FA1*. After 0.3 s, the valve 2 is activated during 0.05 s for changing the pad of *FA1* to a softer state. During this time, valve 1 is deactivated for opening *FA1*. Then, the signals of the valves 1 and 3 are activated for closing the *FA1*, *FB1* and *FB2* during 0.3 s and the pad of *FA1* changes to a tougher state (valve 4 activated) and waits for 0.5 s. This process adapts the pad of the *FA1* to every mango shape. The *P2* starts to collect data. The robot moves the gripper up. The pad of the *FA1* is at tough state and starts an open/close loop (open during 0.05 s, close for 1 s). During this loop, the signals of *ACC1* and *ACC*2 are collected. Then, valve 5 is activated, *P1* is approached to the mango surface and starts to collect data. The whole process is shown in figure 5.

2.5. Signal pre-processing and statistical analysis

The raw spectra from the spectrometer were transformed to apparent absorbance (log (1/R)) values using The Unscrambler Version 10.2 software package (CAMO Software AS, Oslo, Norway) to obtain linear correlations of the NIR values with the concentration of the estimated constituents (Shao *et al.*, 2007; Liu *et al.*, 2009) and centred by subtracting their averages in order to ensure that all results will be interpretable in terms of variation around the mean.

Figure 6 shows raw VNIR and NIR spectra and its correction after the application of the pre-processing methods. Savitzky-Golay smoothing (the segment size is 15) was applied to improve the signal-to-noise ratio in order to reduce the effects caused by the physiological variability of samples (Carr *et al.*, 2005; Beghi *et al.*, 2017). Due to the fruit fresh light scattering (Santos *et al.,* 2013), the light does not always travel the same distance in the sample before it is detected. A longer light traveling path corresponds to a lower relative reflectance value, since more light is absorbed. This causes a parallel translation of the spectra. This kind of variation is not useful for the calibration models and need to be eliminated by the EMSC technique (He *et al.*, 2007; Martens *et al.*, 2003; Bruun *et al.*, 2007). In addition to those three pre-processing, the second derivate with Gap-Segment (2.3) were the best results for the NIR spectra because it allowed the extraction of useful information (Rodriguez-Saona *et al.*, 2001). The different pre-treatments were applied in the sequence explained, specifying that the first two pre-treatments (smoothing and EMSC) were only applied to the VNIR spectra and those two with the third (second derivate) applied to the NIR spectra (Cortés *et al.*, 2016). Finally, the adjustment to the spectral intensities from each sensor ACC1, ACC2, P1 and P2 was range-normalised so the data from all samples were directly comparable to each other (Andrés & Bona, 2005; Blanco *et al.*, 2006).

The different sensor signals were combined through a 'low-level' fusion procedure (Roussel *et al.*, 2003) by concatenating the pre-processed sensor signals - appending one to another- to create a single matrix with a total of 5516 variables, which was processed using The Unscrambler. Data were organised in a matrix where the rows represent the number of samples (#N = 275 samples) and the columns represent the variables (X-variables and Y-variables). The X-variables, or predictors, were the signals obtained by the data fusion between the two fibre-optic probes of the spectrometer and the accelerometers. The Y-variable, or response, was the *RPI* of each sample. In order to correct the relative influences of the different instrumental responses on model, standardisation technique was used, where the weight of each X-variable was the standard deviation of the variable (Bouveresse *et al.*, 1996). Then, fifteen regression models for each combination of the spectra data from the different sensors were developed by partial least squares (PLS) to predict *RPI*. Samples were randomly separated into two groups, 75 % of the samples were used to develop the model that was validated by cross validation, while the remaining samples (25 %) were used as the prediction set. The root mean square error of calibration (RMSEC), root mean squared error of cross validation (RMSECV), the root mean square error of prediction (RMSEP), the coefficient of determination for calibration (R^2_C), for prediction (R^2_P) and for cross validation (R^2_{CV}), and the required number of latent variables (LV) were used to judge the accuracy of the PLS model.

3. RESULTS AND DISCUSSION

3.1. Changes in mango quality during ripening

The changes observed in the physicochemical characteristics (F_{max}, *TSS* and *TA*) of mangoes during postharvest storage are shown in Table 1.

For all sets of mangoes there was a steady decrease in fruit firmness over time starting around 137 N to fell to 28 N. These changes are due to significant changes in the composition and structure of cell walls and middle lamella due to the solubilisation, de-esterification and de-polymerisation of the middle lamella (Singh *et al.*, 2013), and the enzymatic activity (Prasanna *et al.*, 2007; Yashoda *et al.*, 2007). A similar behaviour has been reported for other mango varieties such as 'Alphonso' (Yashoda *et al.*, 2005), 'Ataulfo' (Palafox-Carlos *et al.*, 2012), 'Keitt' (Ibarra-Garza *et al.*, 2015) or 'Osteen' (Cortés *et al.*, 2016). Similarly, the *TA* tends to decrease due to the cell metabolisation of volatile organic acids and non-volatile constituents (Padda *et al.*, 2011), and in addition acids can be used as substrates for respiration when sugars have been consumed or participated in the synthesis of phenolic compounds, lipids and volatile aromas (Abu-Goukh *et al.*, 2010). In contrast, the *TSS* increased continuously during postharvest storage due to the conversion of starch to glucose and fructose, which are used as substrates during fruit respiration (Eskin *et al.*, 2013). Similar results were observed by Quintana *et al.* (1984) who reported that *TSS* of mango increased gradually up to ripeness.

RPI was calculated for every day of storage. Figure 7 shows the evolution of the *RPI* through median plots with 95 % confidence intervals during the storage. It can be observed that the values of the index clearly decreased during ripening. Initially, the *RPI* declines sharply when the fruits ripen to achieve their optimum organoleptic properties, and then, fruit reaches the stage of over ripeness where the curve follows a constant trend because the product reaches a maximum content of *TSS* and minimum firmness and *TA*.

3.2. Non-destructive prediction of mango ripening

The data was concatenated (accelerometers and VIS-NIR spectra) (Decruyenaere *et al.*, 2009; Roussel *et al.*, 2003) to form a representative complex spectrum with a total of 5516 variables. Table 2 shows the results of the validation and prediction results of the PLS models built for the data obtained by every single sensor and for the data fusion (due to the concatenation of wavenumber) performed among all possible combinations of spectral data.

The best PLS model for prediction of *RPI* is presented in the Fig. 8. Figure 9 shows the regression coefficients of the best developed model and the PRESS plot for identifying the optimum number of LVs. The results for this model were obtained using VIS-NIR fibre-optic probes and the two accelerometer signals. The calibration model for predicting the RPI has an R^2_c = 0.945 and RMSEC = 0.235, and the validation of the calibration model has an R^2_{cv} = 0.0.804 and RMSECV = 0.447. The prediction model indicates a good prediction performance, and obtained values of R^2_p = 0.832 and RMSEP = 0.520.

3.3 **Integration of tactile sensing and reflectance data in the robot gripper**

This novel gripper presents an important evolution from other previous grippers for sensing and handling the firmness of eggplants and mangoes by using accelerometers as tactile sensors (Blanes *et al.*, 2015a and 2015b). Unlike these previous grippers that caused damages in some over-ripe mangoes due to the action of a suction cup needed for holding the fruits, this new gripper incorporates four fingers and intrinsic sensors that avoid the need of such suction cup when holding the fruit for measurement and placing.

Besides, the combination of the two probes achieved better results than *P2* or *P1* standalone, having an R^2_p of 0.802 compared to those obtained of 0.732 and 0.632, respectively. In the same way, *ACC1* together with *ACC2* had better result than *ACC1* or *ACC2* alone with an R^2_p of 0.655 compared to 0.444 and 0.300, respectively. It is important to remark that the composition of a fruit is not uniform and hence some parts of the mango may have different ripeness than others. Therefore, it is necessary to take simultaneous measurements at least in the three points studied to obtain reliable and robust results. Blanes *et al.* (2015b) developed a gripper with three accelerometers to estimate the ripeness of mangoes cv. 'Osteen' achieving a R^2_P = 0.760 which is lower than the current robot gripper (R^2_P = 0.832). This highlights the important contribution of the integration of both tactile sensors and VNIR reflectance measurements in the robotic gripper to assess the quality of the mangos during fruit handling.

A handicap of this system in the current version is the long time needed to process every mango. The incorporation of two spectrometer probes increases the processing time of every mango up to 9 s. However, experiments have been done in a first prototype for testing, where the algorithms, hardware and processes were not optimised for working at high speed. Integrating better the hardware, optimising algorithms and parallelising some processes, the whole process could experience a dramatic reduction of the operation speed. On the other hand, the combination of sensors of different nature provides the capability of obtaining simultaneously both mechanical and optical properties of the fruit. This innovative approach is highly interesting in the emerging competitive food sector where monitoring of product quality reproducibility and traceability is decisive in the manufacture (Kondo, 2010).

4. CONCLUSIONS

A novel sensorised robot gripper with two accelerometers and two VIS-NIR reflectance probes, has been developed and tested for fruit handling. The design uses sensors that do not need direct contact, are intrinsic tactile sensors, and can take the measurements simultaneously during the mango handling which is an important advantage over the state of the art. The results show the prediction of the quality of the fruit using the *RPI* through the information given by VIS-NIR spectra and non-destructive impact obtained during handling, achieving an R^2_p of 0.832 and RMSEP of 0.520. This innovative prototype integrates different types of sensors of different nature, whose data information is combined to obtain better prediction. The fusion of different types of sensors like spectrometry (electromagnetic) and accelerometers (vibrational) achieved better results that using only the accelerometers, or similar results than using spectroscopy, but in this case, the measurements were made while the fruit was handled. In this way, results show the potential and advantages of performing simultaneous operations of sensors of different nature integrated on a robot gripper that can inspect and classify the mangoes by their ripeness during a pick and place robot process.

ACKNOWLEDGEMENTS

This work has been partially funded by the Instituto Nacional de Investigación y Tecnología Agraria y Alimentaria de España (INIA) and FEDER through research projects RTA2012-00062-C04-01, RTA2012-00062-C04-02, RTA2012-00062-C04-03, and by the Conselleria d' Educació, Investigació, Cultura i Esport, Generalitat Valenciana, through the project AICO/2015/122. V. Cortés thanks the Spanish MEC for the FPU grant (FPU13/04202).

REFERENCES

Abu-Goukh, A.A., Shattir, A.E., & Mahdi, F.M. (2010). Physico-chemical changes during growth and development of papaya fruit. II: Chemical changes. *Agriculture and Biology Journal of North America*, 2151-7517.

Andrés, J.M. & Bona, M.T. (2005). Analysis of coal by diffuse reflectance near-infrared spectroscopy. *Analytica Chimica Acta*, 535, 123-132.

Beghi, R., Giovenzana, V., Brancadoro, L. & Guidetti, R. (2017). Rapid evaluation of grape phytosanitary status directly at the check point station entering the winery by using visible/near infrared spectroscopy. *Journal of Food Engineering*, 204, 46-54.

Blanco, M., Alcalá, M., González, J.M. & Torras, E. (2006). Near infrared spectroscopy in the study of polymorphic transformations. *Analytica Chimica Acta,* 567, 262-268.

Blanes, C., Cortés, V., Ortiz, C., Mellado, M., & Talens, P. (2015b). Non-destructive assessment of mango firmness and ripeness using a robotic gripper. *Food Bioprocess Technology*, 8, 1914-1924.

Blanes, C., Mellado, M., & Beltrán, P. (2016). Tactile sensing with accelerometers in prehensile grippers for robots. *Mechatronics*, 33, 1-12.

Blanes, C., Ortiz, C., Mellado, M., & Beltrán, P. (2015a). Assessment of Eggplant Firmness with Accelerometers on a Pneumatic Robot Gripper. *Computers and Electronics in Agriculture*, 113, 44–50.

Blasco, J., Aleixos, N. & Moltó, E. (2003). Machine Vision System for Automatic Quality Grading of Fruit. *Biosystems Engineering* 85, 415-423.

Bogue, R. (2009). The role of robots in the food industry: a review. *Industrial Robot: An International Journal*, 36 (6), 531-536.

Bouveresse, E., Hartmann, C., Last, I. R., Prebble, K. A., & Massart, L. (1996). Standardization of Near-Infrared Spectrometric Instruments. *Anal. Chem.*, 68, 982-990.

Bruun, S.W., Sondergaard, I. & Jacobsen, S. (2007). Analysis of protein structures and interactions in complex food by Near-Infrared spectroscopy. 1. Gluten Powder. *J. Agric. Food Chem.*, 55, 7234-7243.

Calatrava, J. (2014). Chapter 2: Mango, Economics and International Trade. *In Mango International Enciclopedia*, Sultanate Of Oman: Royal Court Affairs Ed.

Carr, G.L., Chubar, O. & Dumas, P. (2005). Spectrochemical Analysis Using Infrared Multichannel Detectors 1st edn. (eds., Bhargava, R. & Levin, I.W.) 56–84. Oxford: Wiley-Blackwell.

Cimander, C., & Mandenius, C. (2002). Online monitoring of a bioprocess based on a multi-analyser system and multivariate statistical process modelling. *Journal of Chemical Technology and Biotechnology*, 77 (19), 1157-1168.

Cimander, C., Carlsson, M., & Mandenius, C.F. (2002). Sensor fusion for on-line monitoring of yoghurt fermentation. *Journal of Biotechnology*, 99, 237-248.

Cortés, V., Ortiz, C., Aleixos, N., Blasco, J., Cubero, S., & Talens, P. (2016). A new internal quality index for mango and its prediction by external visible and near-infrared reflection spectroscopy. *Postharvest Biol. Technol.*, 118, 148–158.

Decruyenaere, V., Lecome, Ph., Demarquilly, C., Aufrere, J., Dardenne, P., Stilmant, D. & Buldgen, A. (2009). Evaluation of green forage intake and digestibility in ruminants using near infrared reflectance spectroscopy (NIRS): Developing a global calibration. *Animal Feed Science and Technology*, 148, 138-156.

Eskin, N.A.M., Hoehn, E., & Shahidi, F. (2013). Fruits and vegetables. Eskin, N.A.M., Shahidi, F. (Eds.), *Biochemistry of foods*, 49–126.

Giovannoni, J.J. (2004). Genetic regulation of fruit development and ripening. *Plant Cell*, 16, 170–180.

He, Y., Li, X. & Deng, X. (2007). Discrimination of varieties of tea using near infrared spectroscopy by principal component analysis and BP model. *Journal of Food Engineering*, 79, 1238-1242.

Hernández, Y., Lobo, M.G., & González, M. (2006). Determination of vitamin C in tropical fruits: a comparative evaluation of methods. *Food Chem.*, 96 (4), 654–664.

Huang, X., Xu, H., Wu, L., Dai, H., Yao, L., & Han, F. (2016). A data fusion detection method for fish freshness based on computer vision and near-infrared spectroscopy. *Analytical Methods*, 8, 2929-2935.

Ibarra-Garza, I.P., Ramos-Parra, P.A., Hernández-Brenes, C., & Jacobo-Velázquez, D.A. (2015). Effects of postharvest ripening on the nutraceutical and physicochemical properties of mango (Mangifera indica L. cv Keitt). *Postharvest Biology and Technology*, 103, 45-54.

Ignat T., Alchanatis, V. & Schmilovitch. Z. (2015). Maturity prediction of intact bell peppers by sensor fusion. *Chemical Engineering Transactions*, 44, 67-73.

Jha, S.N., Chopra, S., & Kingsly, A.R.P. (2007). Modeling of color values for non-destructive evaluation of maturity of mango. *J. Food Eng.*, 78, 22–26.

Jha, S.N., Jaiswal, P., Narsaiah, K., Sharma, R., Bhardwaj, R., Gupta, M., & Kumar, R. (2013). Authentication of mango varieties using near infrared spectroscopy. *Agric. Res.*, 2 (3), 229-235.

Kienzle, S., Sruamsiri, P., Carle, R., Sirisakulwat, S., Spreer, W., & Neidhart, S. (2011). Harvest maturity specification for mango fruit (Mangiferaindica L. 'Chok Anan') in regard to long supply chains. *Postharvest Biol. Technol.*, 61, 41–55.

Kondo, N. (2010). Automation on fruit and vegetables grading system and food traceability. *Trends in Food Science & Technology*, 21, 145-152.

Lee, M. H., & Nicholls, H. R. (1999). Tactile sensing for mechatronics – a state of the art survey. *Mechatronics*, 9, 1-31.

Liu, F., Jiang, Y., & He, Y. (2009). Variable selection in visible/near infrared spectra for linear and nonlinear calibrations: A case study to determine soluble solids content of beer. *Analytica Chimica Acta*, 635, 45-52.

Luke, H. (2013). 'The Economics of the Mango Trade'. Examining the economic impact of globally traded mangoes. University of Minnesota-Duluth Economics. PDF File: https://www.mcee.umn.edu/sites/mcee.umn.edu/files/heine-cloquet_high_school001-for_website.pdf

Martens, H., Nielsen, J. P. & Engelsen, S. B. (2003). Light scattering and light absorbance separated by extended multiplicative signal correction. Application to near-infrared transmission analysis of powder mixtures. *Anal. Chem.*, 75, 394-404.

Mercadante, A.Z., & Rodriguez-Amaya, D.B. (1998). Effects of ripening, cultivar differences, and processing on the carotenoid composition of mango. *J. Agric. Food Chem.*, 46 (1), 128–130.

Nicolaï, B.M., Beullens, K., Bobelyn, E., Peirs, A., Saeys, W., Theron, I.K., & Lammertyn, J. (2007). Non-destructive measurement of fruit and vegetable quality by means of NIR spectroscopy: a review. *Postharvest Biol. Technol.*, 46, 99–118.

Ornelas-Paz, J.D.J., Yahia, E.M., & Gardea-Bejar, A.A. (2008). Changes in external and internal color during postharvest ripening of 'Manila' and 'Ataulfo' mango fruit and relationship with carotenoid content determined by liquid chromatography–APcI+-time-of-flight mass spectrometry. *Postharvest Biol. Technol.*, 50 (2), 145–152.

Padda, S.M., do Amarante, C.V.T., Garcia, R.M., Slaughter, D.C., & Mitcham, E.M. (2011). Methods to analyze physicochemical changes during mango ripening: a multivariate approach. *Postharvest Biol. Technol.*, 62, 267–274.

Palafox-Carlos, H., Yahia, E., Islas-Osuna, M.A., Gutierrez-Martinez, P., Robles-Sánchez, M., & González-Aguilar, G.A. (2012). Effect of ripeness stage of mango fruit (Mangifera indica L., cv. Ataulfo) on physiological parameters and antioxidant activity. *Sci. Hort.*, 135 (0), 7–13.

Prasanna, V., Prabha, T.N., & Tharanathan, R.N. (2007). Fruit ripening phenomena- an overview. *Crit. Rev. Food Sci. Nutr.*, 47, 1–19.

Quintana, E.G, Nanthachai, P., Hiranpradit, H., Mendoza, D. B., & Ketsa, S. (1984). Changes in mango during growth and maturation: Growth and development of mango. *ASEAN Food Handling Bureau*, 21–27.

Rodriguez-Saona, L.E., Fry, F.S., McLaughlin, A. & Calvey, E.M. (2001). Rapid analysis of sugars in fruit juices by FT-NIR spectroscopy. *Carbohydrate Research*, 336, 63-74.

Roussel, S., Bellon-Maurel, V., Roger, J. M., & Grenier, P. (2003). Fusion of aroma, FT-IR and UV sensor data bsed on the Bayesian inference. Application to the discrimination of white grape varieties. *Chemometrics and Intelligent Laboratory Systems*, 65 (2), 209-219.

Roussel, S., Bellon-Maurel, V., Roger, J.M. & Grenier, P. (2003). Authenticating white grape must variety with classification models based on aroma sensors, FT-IR and UV spectrometry. *Journal of Food Engineering*, 60, 407-419.

Santos, J., Trujillo, L.A., Calero, N., Alfaro, M.C., & Muñoz, J. (2013). Physical characterization of a commercial suspoemulsion as a reference for the development of suspoemulsions. *Chem. Eng. Technol.*, 11, 1–9.

Schmilovitch, Z., Mizrach, A., Hoffman, A., Egozi, H., & Fuchs, Y. (2000). Determination of mango physiological indices by near-infrared spectrometry. *Postharvest Biol. Technol.*, 19 (3), 245–252.

Shao, Y., He, Y., Gómez, A.H., Pereir, A.G., Qiu, Z., & Zhang, Y. (2007). Visible/near infrared spectrometric technique for nondestructive assessment of tomato ‘Heatwave’ (Lycopersicumesculentum) quality characteristics. *J. Food Eng.*, 81 (4), 672–678.

Singh, Z., Singh, R.K., Sane, V.A., & Nath, P. (2013). Mango–Postharvest biology and biotechnology. *Crit. Rev. Plant Sci.*, 32 (4), 217–236.

Steinmetz, V., Roger, J. M., Moltó, E., & Blasco, J. (1999). On-line fusion of colour camera and spectrophotometer for sugar content prediction of apples. *Journal of Agricultural Engineering Research*, 73 (2), 207-216.

Tai, K., El-Sayed, A. R., Shahriari, M., Biglarbegian, M., & Mahmud, S. (2016). State of the art robotic grippers and applications. *Robotics*, 5 (2), 11.

Theanjumpol, P., Self, G., Rittiron, R., Pankasemsu, T., & Sardsud, V. (2013). Selecting variables for near infrared spectroscopy (NIRS) evaluation of mango fruit quality. *J. Agric. Sci.*, 5 (7), 146-159.

Torres, R., Montes, E.J., Perez, O.A., & Andrade, R.D. (2013). Relación del color y del estado de madurez con las propiedades fisicoquímicas de frutas tropicales. *Información Tecnológica*, 24 (4), 51.

Ulloa, P. A., Guerra, R., Cavaco, A. M., Rosa da Costa, A. M., Figueira, A. C., & Brigas, A. F. (2013). Determination of the botanical origin of honey by sensor fusion of impedance e-tongue and optical spectroscopy. *Computers and Electronics in Agriculture*, 94, 1-11.

Vásquez-Caicedo, A.L., Sruamsiri, P., Carle, R., & Neidhart, S. (2005). Accumulation of all-trans-b-carotene and its 9-cis and 13-cis stereoisomers during postharvest ripening of nine Thai mango cultivars. *J. Agric. Food Chem.*, 53, 4827–4835.

Vélez-Rivera, N., Blasco, J., Chanona-Pérez, J., Calderón-Domínguez, G., Perea-Flores, M.J., Arzate-Vázquez, I., Cubero, S., & Farrera-Rebollo, R. (2014b). Computer vision system applied to classification of ‘Manila' mangoes during ripening process. *Food Bioprocess Technol.*, 7, 1183–1194.

Vélez-Rivera, N., Gómez-Sanchis, J., Chanona-Pérez, J., Carrasco, J.J., Millán-Giraldo, M., Lorente, D., Cubero, S., & Blasco, J. (2014a). Early detection of mechanical damage in mango using NIR hyperspectral images and machine learning. *Biosyst. Eng.*, 122, 91–98.

Wilson, M. (2010). Developments in robot applications for food manufacturing. *Industrial Robot: An International Journal*, 37 (6), 498-502.

Yashoda, H.M., Prabha, T.N., & mTharanathan, R.N. (2007). Mango ripening—role of carbohydrases in tissue softening. *Food Chem.*, 102 (3), 691–698.

Yashoda, H.M., Prabha, T.N., & Tharanathan, R.N. (2005). Mango ripening—chemical and structural characterization of pectic and hemicellulosic polysaccharides. *Carbohydr. Res.*, 340 (7), 1335–1342.

Zakaria, A., Shakaff, A.Y.M., Masnan, M.J., Saad, F.S.A., Adom, A.H., Ahmad, M.N., & Kamarudin, L.M. (2012). Improved maturity and ripeness classifications of magnifera indica cv. harumanis mangoes through sensor fusion of an electronic nose and acoustic sensor. *Sensors*, 12 (5), 6023–6048.

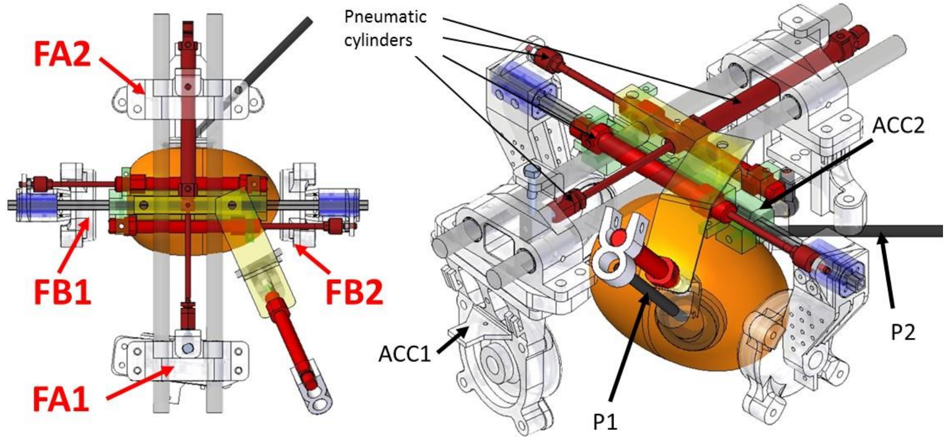
FA2
FB1
FB2
FA1
Pneumatic
cylinders
ACC2
ACC1
P1
P2

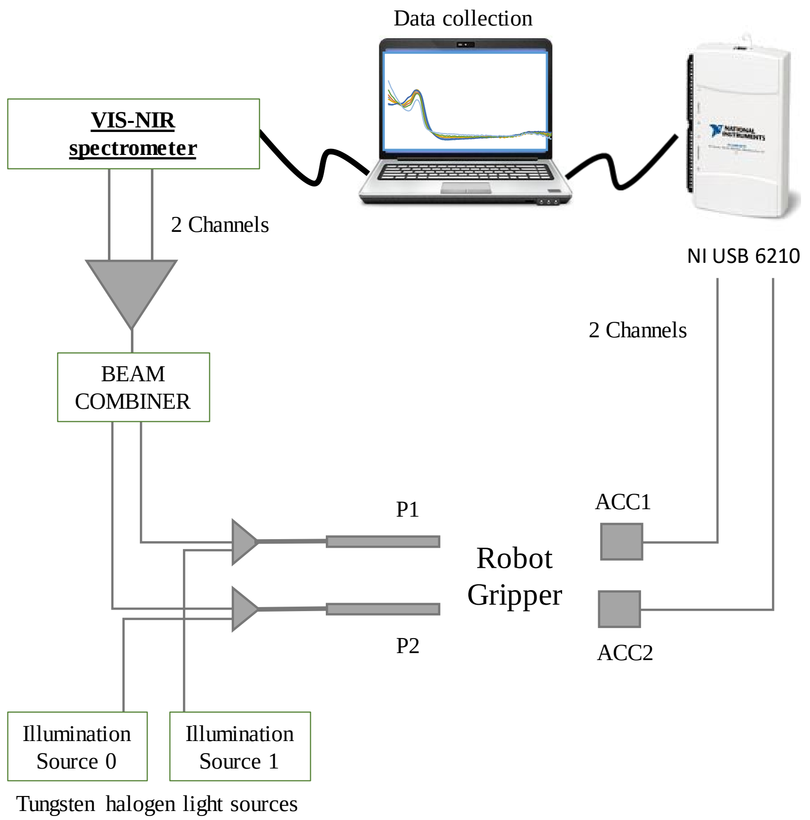
Data collection
VIS-NIR
spectrometer
2 Channels
NI USB 6210
2 Channels
BEAM
COMBINER
P1
ACC1
Robot
Gripper
P2
ACC2
Illumination
Source 0
Illumination
Source 1
Tungsten halogen light sources

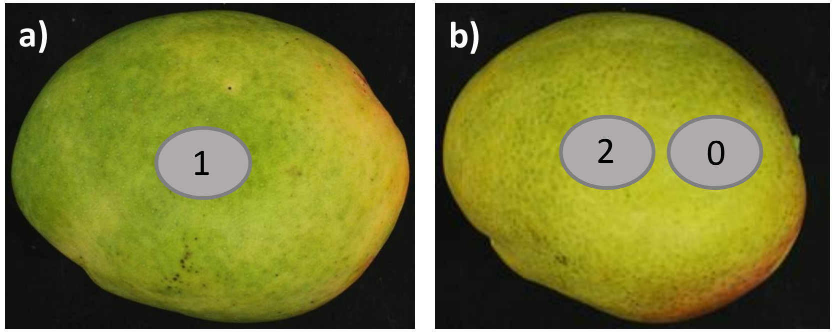
a)
1
b)
2
0

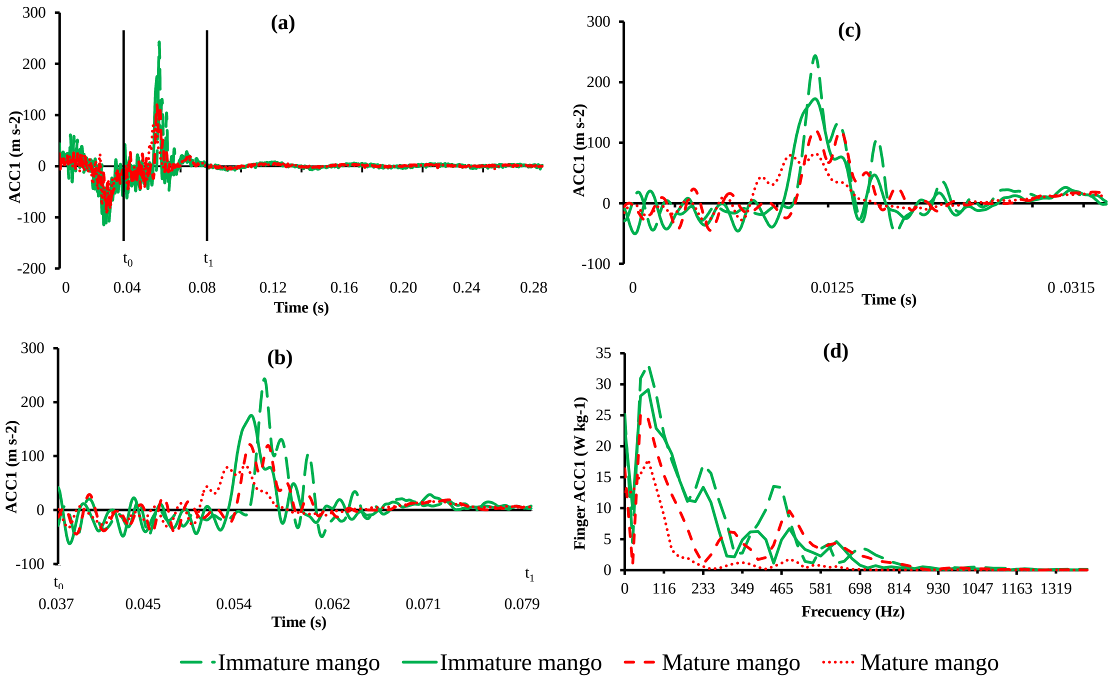

(a)
(b)
(c)
(d)
ACC1 (m s-2)
Time (s)
Finger ACC1 (W kg-1)
Frecuency (Hz)
t0
t1
Immature mango
Immature mango
Mature mango
Mature mango

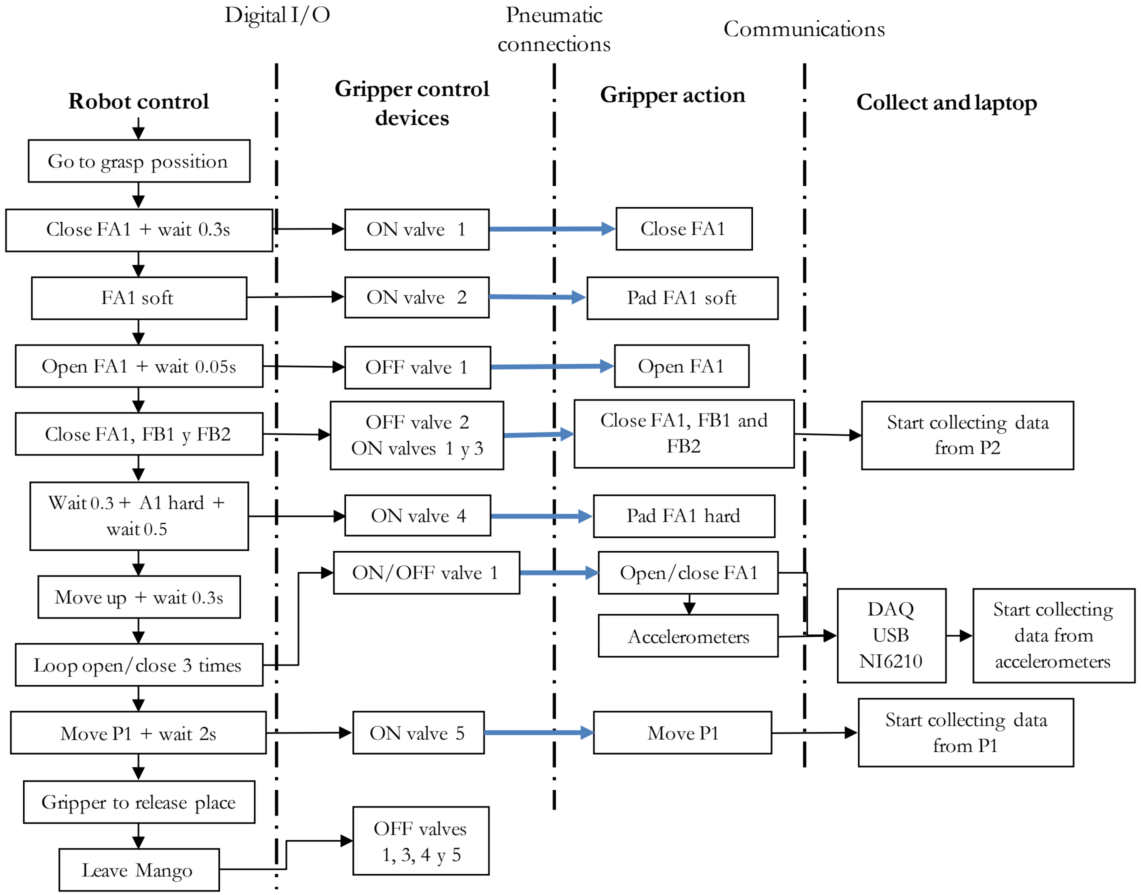

Digital I/O
Pneumatic connections
Communications
Robot control
Gripper control devices
Gripper action
Collect and laptop
Go to grasp possition
Close FA1 + wait 0.3s
ON valve 1
Close FA1
FA1 soft
ON valve 2
Pad FA1 soft
Open FA1 + wait 0.05s
OFF valve 1
Open FA1
Close FA1, FB1 y FB2
OFF valve 2
ON valves 1 y 3
Close FA1, FB1 and FB2
Start collecting data from P2
Wait 0.3 + A1 hard + wait 0.5
ON valve 4
Pad FA1 hard
ON/OFF valve 1
Open/close FA1
Move up + wait 0.3s
Accelerometers
DAQ USB NI6210
Start collecting data from accelerometers
Loop open/close 3 times
Move P1 + wait 2s
ON valve 5
Move P1
Start collecting data from P1
Gripper to release place
Leave Mango
OFF valves 1, 3, 4 y 5

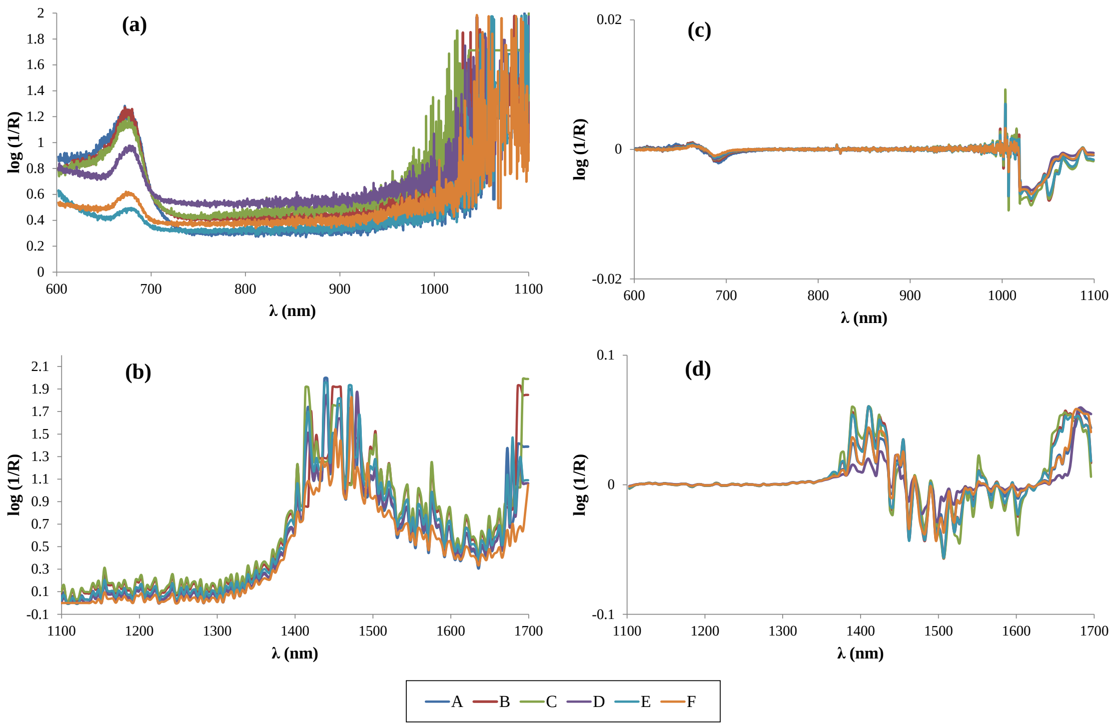
(a)
log (1/R)
λ (nm)
(b)
log (1/R)
λ (nm)
(c)
log (1/R)
λ (nm)
(d)
log (1/R)
λ (nm)
A
B
C
D
E
F

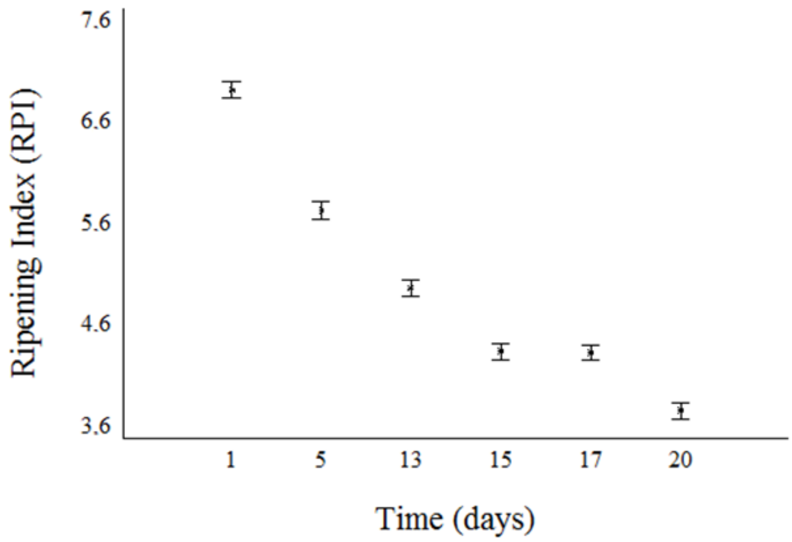

Ripening Index (RPI)
7.6
6.6
5.6
4.6
3.6
1
5
13
15
17
20
Time (days)

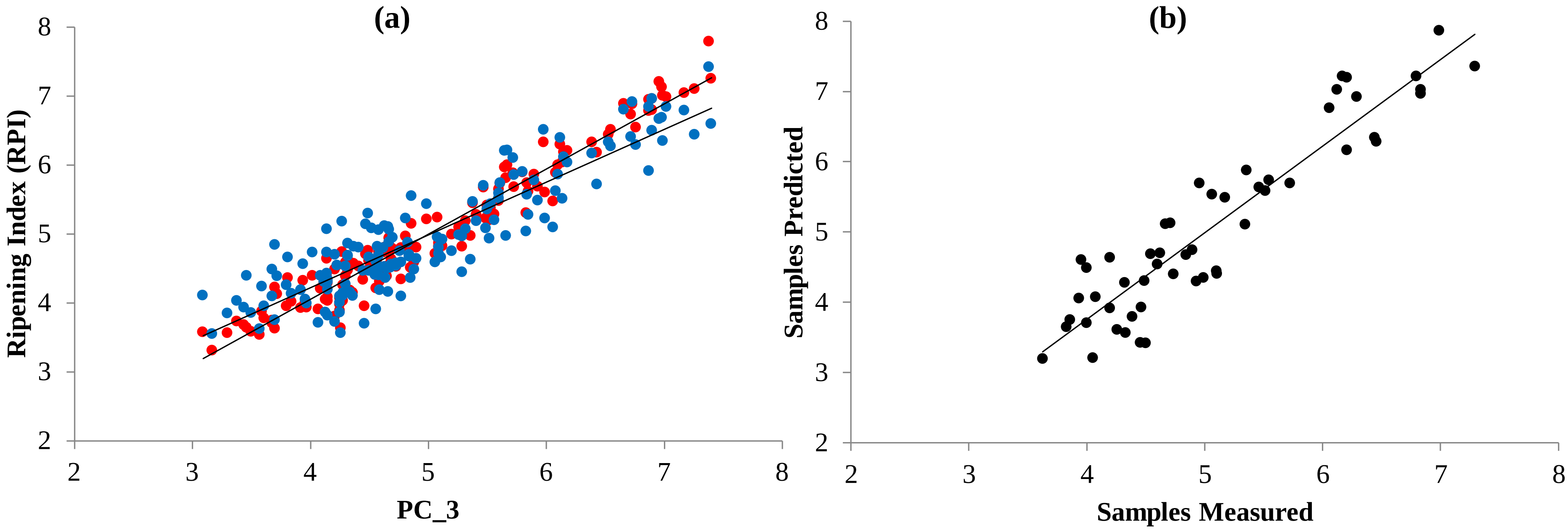
(a)
(b)
Ripening Index (RPI)
PC_3
Samples Predicted
Samples Measured
2
3
4
5
6
7
8

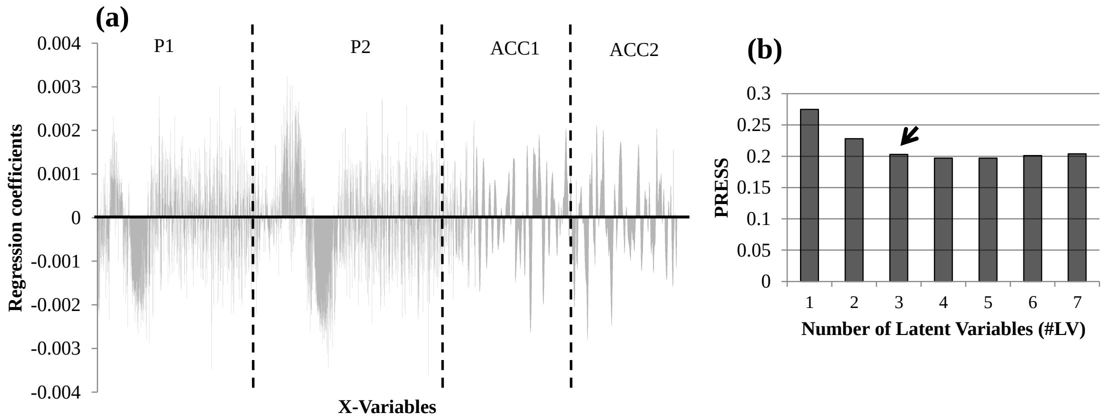

(a)
P1
P2
ACC1
ACC2
0.004
0.003
0.002
0.001
0
-0.001
-0.002
-0.003
-0.004
Regression coefficients
X-Variables
(b)
0.3
0.25
0.2
0.15
0.1
0.05
0
PRESS
1
2
3
4
5
6
7
Number of Latent Variables (#LV)

Table 1. Descriptive statistics for the quality parameters analysed in mango samples during the storage period.

		Set A	*Set B*	*Set C*	*Set D*	*Set E*	*Set F*
Mechanical properties	F_{max} (N)	137 ± 18^{a}	62 ± 16^{b}	45 ± 16^{c}	34 ± 11^{d}	35 ± 8^{d}	28 ± 8^{e}
Internal composition	*TSS (%)*	10.4 ± 0.9^{a}	$12\pm1^{b,c}$	$12\pm1^{c,d}$	12 ± 1^{d}	12 ± 1^{b}	$12\pm2^{b,c}$
	TA (%)	0.8 ± 0.2^{a}	0.62 ± 0.15^{b}	0.41 ± 0.08^{c}	0.30 ± 0.06^{d}	0.29 ± 0.06^{d}	0.19 ± 0.05^{e}

Values are mean ± SD.
a–e Different superscripts in the same row indicate significant difference among sets ($p < 0.05$).

Table 2. Comparison of the prediction of mango ripening provided by different possible combination of sensor fusion to the two fibre-optic probes of VIS-NIR spectrometer and two accelerometers located at the fingers of the robot gripper.

		Calibration set				Prediction set	
Sensors	**#LV**	**R^2_C**	**RMSEC**	**R^2_{CV}**	**RMECV**	**R^2_P**	**RMSEP**
P2	1	0.769	0.506	0.742	0.537	0.732	0.663
P1	3	0.895	0.323	0.739	0.512	0.632	0.727
P2+ P1	3	0.933	0.268	0.782	0.487	0.802	0.554
ACC1	6	0.677	0.574	0.575	0.663	0.444	0.871
ACC2	4	0.611	0.626	0.48	0.727	0.300	1.020
ACC1 + ACC2	4	0.758	0.758	0.595	0.595	0.655	0.737
P2+ ACC1	2	0.854	0.373	0.77	0.471	0.778	0.613
P2+ ACC2	1	0.695	0.586	0.649	0.632	0.733	0.665
P1 + ACC1	4	0.940	0.251	0.753	0.513	0.662	0.698
P1 + ACC2	5	0.971	0.175	0.776	0.493	0.662	0.742
P2 + P1 + ACC1	4	0.973	0.166	0.786	0.467	0.797	0.550
P2 + P1 + ACC2	2	0.867	0.379	0.777	0.494	0.784	0.595
P2 + ACC1 + ACC2	2	0.813	0.460	0.705	0.580	0.813	0.567
P1 + ACC1 + ACC2	5	0.971	0.176	0.779	0.490	0.733	0.642
P2 + P1 + ACC1 + ACC2	3	0.945	0.235	0.804	0.447	**0.832**	0.520